Published in final edited form as:
Dev Dyn. 2007 December ; 236(12): 3393–3401. doi:10.1002/dvdy.21235.

In Vivo Quantum Dot Labeling of Mammalian Stem and Progenitor Cells

Jonathan R. Slotkin[1,2], **Lina Chakrabarti**[3], **Hai Ning Dai**[1], **Rosalind S.E. Carney**[1,3], **Tsutomu Hirata**[1,3], **Barbara S. Bregman**[1], **G. Ian Gallicano**[4], **Joshua G. Corbin**[1,3], and **Tarik F. Haydar**[3,*]

1*Department of Neuroscience, Georgetown University School of Medicine, Washington, DC*

2*Department of Neurosurgery, The Brigham and Women's Hospital, The Children's Hospital, Harvard Medical School, Boston, Massachusetts*

3*Center for Neuroscience Research, Children's Research Institute, Children's National Medical Center, Washington, DC*

4*Department of Cell Biology, Georgetown University School of Medicine, Washington, DC*

Abstract

Fluorescent semiconductor nanocrystal quantum dots (QDs) are a class of multifunctional inorganic fluorophores that hold great promise for clinical applications and biomedical research. Because no methods currently exist for directed QD-labeling of mammalian cells in the nervous system in vivo, we developed novel in utero electroporation and ultrasound-guided in vivo delivery techniques to efficiently and directly label neural stem and progenitor cells (NSPCs) of the developing mammalian central nervous system with QDs. Our initial safety and proof of concept studies of one and two-cell QD-labeled mouse embryos reveal that QDs are compatible with early mammalian embryonic development. Our in vivo experiments further show that in utero labeled NSPCs continue to develop in an apparent normal manner. These studies reveal that QDs can be effectively used to label mammalian NSPCs in vivo and will be useful for studies of in vivo fate mapping, cellular migration, and NSPC differentiation during mammalian development.

Keywords

quantum dots; stem cells; development; central nervous system

INTRODUCTION

Quantum dots (QDs) are a recently developed class of highly stable, nano-meter-sized inorganic fluorophores (Gao et al., 2004; Medintz et al., 2005; Michalet et al., 2005; Stroh et al., 2005). QDs have significant advantages compared with traditional organic fluorophores, including size-tun-able emission, increased quantum efficiency, broader absorption spectra, narrower emission spectra (i.e., smaller full-width half-maximum), and remarkable resistance to photo bleaching (Bruchez et al., 1998; Chan and Nie, 1998; Han et al., 2001; Jaiswal and Simon, 2004; Rieger et al., 2005). QDs may also be superior to conventional fluorophores in fluorescence resonance energy transfer (FRET) experiments, where there is transfer of energy

*Correspondence to: Tarik F. Haydar, Center for Neuroscience Research, Children's Research Institute, Children's National Medical Center, Washington, DC 20010. E-mail: E-mail: thaydar@cnmcresearch.org.
Drs. Slotkin and Chakrabarti contributed equally to this work.

from a donor to an acceptor fluorophore. In such experiments, QDs may have the ability to function as "molecular beacons," performing biologic sensor functions and also reporting states of protein or molecular conformation (Clapp et al., 2006). In vitro studies have shown that QDs can be targeted to specific intracellular components, can function as cell lineage tracing agents because they are persistent within daughter cell populations, and are photostable for prolonged periods after tissue fixation. QDs also have great potential for extended timelapse imaging studies that involve repeated fluorescence excitation (Rieger et al., 2005).

In addition to their unique optical properties, QDs have the capacity to be functionalized by means of cross-linking with proteins, streptavidin, antibodies, or other bioactive molecules (Michalet et al., 2005; Pathak et al., 2006). This cross-linking may allow QDs to be targeted to specific tissues, cell types, or intracellular organelles. The optical advantages of QDs compared with conventional organic fluorophores promise to greatly improve techniques for labeling and tracking cells both in vitro and in vivo.

Several recent studies have taken advantage of the unique characteristics of QDs to explore their potential for both basic research and clinical applications. One such area is in the study of tumor cell tracking and detection. Several studies have shown that multiple-spectra QDs can be used to achieve coincident tracking of multiple tumor cells in vivo using fluorescence emission-scanning microscopy (Gao et al., 2004; Jaiswal et al., 2004). In the central nervous system, microangiography of deep brain blood vessels and nonspecific labeling of brain cells has been achieved following QD injection into arterial blood (Levene et al., 2004; Voura et al., 2004).

Studies in which QDs have been functionalized with specific antibodies or proteins have also revealed several novel in vitro cell biological applications (Pathak et al., 2006). These include the linking of QDs with receptor ligands (Rosenthal et al., 2002; Dahan et al., 2003; Vu et al., 2005) to track cell migration and diffusion of cell surface receptors (for example the tracking of glycine receptor internalization), and the use of QDs to label organelles (Hoshino et al., 2004) and cytoskeletal components (Nan et al., 2005). It has also been shown that functionalized QDs can impact cell behavior. For example, QDs coated with nerve growth factor (NGF) promote neurite outgrowth in vitro in a manner similar to exogenously applied NGF (Vu et al., 2005). Moreover, QD labeling of both *Xenopus* (Dubertret et al., 2002) and zebrafish (Rieger et al., 2005) embryos have shown that QD injection can be used as a novel method to indelibly label and track developing cells in the nonmammalian vertebrate embryo.

Despite the above-described analyses, methods to safely and efficiently label mammalian stem and progenitor cells in vivo have, to date, been elusive. In this study, we developed two techniques to directly label NSPCs with QDs in vivo. Using in utero ultrasound-guided injection or electroporation, we successfully QD-labeled ventricular zone (VZ) and subventricular zone (SVZ) NSPCs of the mouse embryonic telencephalon in vivo. After quantum dot labeling, NSPCs appear to continue to develop, migrate, and differentiate normally as assayed in vivo until embryonic day (E) 18.5, and in neurosphere assays in vitro. Furthermore, we reveal that QD labeling of early mouse embryos can be used to mark developing cell populations over time. Taken together, these techniques establish a novel approach for the study of the developing mammalian embryo and CNS.

RESULTS

Properties of Quantum Dots

The QDs used were cadmium/selenide (Cd/Se) core, zinc sulfide (ZnS) shell, 10- to 20-nm-diameter water-soluble QDs with a surface phospholipid coating (Type II EviDots, Evident Technologies, Troy, NY; Fig. 1A). To measure QD spectral characteristics using multiphoton

excitation, Neuro2a (N2a) neuroblastoma cells were loaded in vitro with an equimolar mix of 490-nm, 520-nm, 580-nm, and 620-nm carboxy (COOH)-functionalized QDs (~30% saturation of the moiety) by lipofection. Twenty-four hours after loading, the cells were imaged using an infrared pulse laser tuned to 800 nm. The emission fingerprints (Fig. 1B,C) demonstrated that each of the four QD varieties could be distinguished in a single scan using one excitation wavelength. This result confirms that multiphoton excitation at 800 nm is ideal for multiplex QD imaging (Larson et al., 2003) and again demonstrates that the broad absorption and narrow emission profiles of QDs can be exploited for multiple-color labeling of cells in vitro.

Long-term labeling of cells with organic fluorophores [such as green fluorescent protein (GFP) variants] in vivo is often hampered by the silencing of promoters and by photobleaching and extinction during repetitive excitation. To confirm whether optical properties of QDs are more robust than organic probes (Wu et al., 2003) and may, therefore, better facilitate long-term live imaging and tracking of mammalian cells in vivo, we measured the variation of fluorescence intensity over time in viable N2a cells cotransfected with 620-nm QDs and farnesylated enhanced green fluorescence protein (EGFP-F) plasmid. While 2 min of repetitive scanning bleached the membrane-bound EGFP, the QD emission strikingly persisted throughout the experiment, despite that the peak irradiance for the QD excitation line was higher (560 mW/mm^2) than the irradiance for the EGFP line (368 mW/mm^2; Fig. 1D,E; Supplementary Movie S1, which can be viewed at http://www.interscience.wiley.com/jpages/1058-8388/suppmat). These data suggest that QDs can withstand repetitive scanning at high incident power levels and persist longer than organic molecules.

Toxicity Assays: In Vitro and In Vivo

A critical defining characteristic of NSPCs is their capacity to differentiate into mature nervous system cell lineages. To determine whether QD labeling has any adverse effect on NSPC differentiation, we QD-labeled neurosphere-derived NSPCs and tracked their differentiation in vitro. Before differentiation, neurospheres isolated from the ventral telencephalon of embryonic day (E) 14.5 mice were passaged twice and then dissociated into a single cell suspension and loaded with COOH-functionalized 620-nm QDs. After 7 days of differentiation, the cells were immunostained for nestin (to label stem cells), βIII-tubulin (neurons), glial fibrillary acidic protein (GFAP; astrocytes), and NG2 (oligodendrocyte progenitors; Fig. 1G–J). After QD loading, NSPCs retained the capacity to differentiate into proper proportions of all three classes of mature cells (Fig. 1F). Moreover, QD-labeled cells remained stably labeled in vitro for 10 further days without any detectable effect on their morphology or survival (Supplementary Figure S1). This novel demonstration reveals that QD loading does not interfere with the ability of NSPCs to differentiate into the mature neuronal and glial lineages of the mammalian nervous system.

The majority of in vitro studies to date have not found any adverse effects of QDs on cell viability, morphology, or function (Ballou et al., 2004; Jaiswal et al., 2004; Kim et al., 2004) provided the QDs were capped by both ZnS and hydrophilic shells. However, it has been shown that surface modifications can modulate the biocompatibility of QDs used in certain applications (Shiohara et al., 2004; Kirchner et al., 2005). We used lactic acid dehydrogenase (LDH) release and reactive oxygen cytotoxicity assays to investigate whether cells loaded with carboxy-functionalized QD could survive and function normally. When compared with the QD-negative control cultures, cell survival and oxidative stress were found to be normal in the QD-loaded cells (Supplementary Figure S1), suggesting that loading with functionalized QDs does not cause any deleterious effect on cell survival in vitro.

Although QD studies on *Danio rerio* (Rieger et al., 2005) and *Xenopus* (Dubertret et al., 2002) embryos have demonstrated a lack of apparent deleterious effects on embryonic

development in nonmammalian vertebrates, the use of QDs in the mammalian embryonic environment has not been studied. To determine whether QD labeling may be deleterious to the early stages of mammalian development, we directly injected one- and two-cell stage mouse embryos with a range of quantities (0.2–0.02 femtograms) of 520-nm and 620-nm QDs in vitro and allowed them to divide for 1–2 days in culture (Fig. 2A,B, Supplementary Tables S1 and S2). We found that survival of the QD-injected embryos was concentration-dependent: two-cell embryos injected with >0.04 femtograms into a single blastocyst did not progress to the next division, whereas blastocysts receiving 0.04–0.02 femtograms survived well in vitro. Over the course of these experiments, cell divisions in this latter group occurred on schedule and four- and eight-cell stage QD-containing embryos (n = 14) developed normally (Fig. 2C,D). There was a compartmentalized segregation of QDs into daughter cells; in two-cell embryos where each of the two parent cells was injected with a different color QD (n = 10), we found that progeny-specific segregation of QDs during subsequent cell divisions resulted in differently labeled planar caps. Furthermore, both 520-nm and 620-nm QDs were spectrally separated by a single excitation at 800 nm (Fig. 2E). Laser-scanning microscopy enabled three-dimensional (3D) reconstruction of the viable maturing embryos (Movie 2 in Supporting Material online).

To determine whether QD-loaded embryos (n = 225) were capable of longer-term development, we transplanted them into pseudo-pregnant dams at the one- and two-cell stage and recovered viable fetuses at E9.5, E10.5, E11.5, and E13.5 (Fig. 2F–I; Supplementary Table S2). Of interest, QDs were found in all fetal tissues arising from injected one-cell embryos, although some tissues appeared more heavily labeled than others. For example, an E10.5 fetus derived from a one-cell stage embryo injected with 520-nm QD contained more QDs in the umbilical region than the underlying epithelial cells (Fig. 2F,G). Similarly, cells in the ventricular pericardium of an E9.5 fetus labeled with 620-nm QD possessed much higher labeling than other neighboring tissues (Fig. 2H). We also found that fetuses grown from two-cell embryos in which only one blastocyst was labeled with QDs exhibited approximately 50% of their body tissues labeled with QDs. For example, an E11.5 embryo in which only one cell was labeled at the two-cell stage contained QDs in the liver, cardiac primordium, thymus, and hindbrain but lacked detectable QDs in other body tissues. It is important to note that detectable levels of QDs were found in fetal tissues following 9–14 days of embryonic development, despite the many rounds of cell division that successively dilute the QD concentration in labeled cells.

Together, these results demonstrate that QDs are suitable for early mammalian embryonic labeling studies as they do not grossly interfere with early embryogenesis, or with continued fetal development. This type of early embryonic analysis may be particularly useful for future studies on embryonic polarity and mosaicism and to visualize and fate map the formation of nascent primordial layers in mammals.

Direct In Utero Labeling of Neural Cells With Quantum Dots

Using ultrasound guided biomicroscopy (UBM) injection and in utero electroporation, we developed two methods to directly load QDs into NSPCs in the developing embryonic mouse brain. Using UBM as a guide, 620-nm COOH-conjugated QDs were injected into the parenchyma of the caudal ganglionic eminence (CGE) of the ventral telencephalon of E13.5 mouse embryos (Fig. 3A). After 5 further days of in utero survival (i.e., at E18.5), QDs were found in each of the three principle cell types generated by NSPCs; GFAP+ astrocytes, NG2 + oligodendrocyte progenitors, and βIII-tubulin + neurons (Fig. 3B–D; Supplementary Movie S3). Moreover, QD-labeled cells were found substantial distances away from the initial site of injection. These results suggest that QD loading of NSPCs in vivo did not inhibit their migration or subsequent differentiation during the developmental period studied.

We also used in utero electroporation to QD-label NSPCs in viable mouse embryos. The ventricular neuroepithelium of E14.5 mouse embryos was coelectroporated with a mix of 620-nm COOH-functionalized QDs and EGFP-F plasmid (Fig. 3E). Twenty-four hours after electroporation, laser-scanning microscopy revealed moderately efficient QD labeling in VZ and SVZ cells lining the lateral ventricle (Fig. 3F–H). Because the GFP transfection efficiency was greater than that found with the QDs, we hypothesized that the QDs may not have been carrying an adequate charge potential to be sufficiently propelled by electroporation. Therefore, to optimize the QD electroporation, we modified the QDs to increase their negative charge by saturating their phospholipid coats with carboxyl groups. Using agarose gel electrophoresis, we indeed found that the COOH-functionalized QDs we initially used for electroporation (30% saturation by the COOH groups) were effectively neutral in charge. In contrast, fully COOH-saturated QDs had a net negative charge and migrated more efficiently toward the anode during electrophoresis (Fig. 3I). This modification dramatically increased the labeling efficiency of neuroepithelial cells in the developing mouse nervous system, with COOH-saturated QDs robustly labeling the neural precursor cells. This enabled 3D reconstruction of QD-loaded VZ and SVZ neural precursor cells in situ using multiphoton imaging (Fig. 3J–M).

DISCUSSION

QDs have significant optical advantages compared with conventional organic fluorophores and promise to greatly improve techniques for labeling and tracking cells both in vitro and in vivo. In vitro work on nervous system tissue and in vivo applications outside of the nervous system have shown that QDs can be used as stable inorganic fluorophores for biologic research applications and potential human clinical use (Michalet et al., 2005; Pathak et al., 2006). However, the ability of mammalian embryos and nervous system cells to take up quantum dots in vivo has not been demonstrated and has been a major obstacle for rapid application of these new tools for mammalian developmental and in vivo cell labeling studies. We have developed two techniques to directly QD-label NSPCs in the mouse embryonic telencephalon in vivo, and have thus established a novel approach for the study of mammalian nervous system development. In this study, we have demonstrated the efficacy of QD labeling of NSPCs and embryos both in vitro and in vivo and have shown in the embryonic periods studied that QD labeling does not appear to negatively impact the ability of such cells to survive, migrate, and differentiate into all mature nervous system lineages. These novel and reliable methods for directly labeling NSPCs with QDs in vivo also demonstrate that surface modification can dramatically improve electroporation cell labeling efficiency. We also establish that QDs do not appear to be toxic to mammalian NSPCs in vitro, in vivo, and during the initial steps of mammalian embryonic development.

Applications of QDs

One of the greatest potential uses of QDs is for the specific detection of diseased cells that express unique markers and the delivery of therapeutic molecules to diseased tissue by means of coating with therapeutic molecules (Michalet et al., 2005). QDs may possess significant advantages over current methods to label transplanted cells, which have been hampered by both safety issues (e.g., the use of engineered viruses as vectors) and the ability of cells to reliably and permanently express a given factor (e.g., the use of liposomes or naked DNA). Experiments outside of the nervous system have demonstrated that QDs may be superior in certain human diagnostic clinical applications such as the identification of tumor-positive sentinel lymph nodes (Kim et al., 2004; Soltesz et al., 2005, 2006). Our in vivo demonstration of the lack of toxicity using the developing embryo and nervous system support the further exploration of QDs as diagnostic and therapeutic tools for human disease.

Our in vitro analyses also confirm that certain optical properties of QDs may facilitate experimental approaches that are difficult to achieve with organic fluorophores. In particular, QDs possess broad absorption spectra and sharply defined emission spectra. Together, these spectral characteristics enable simultaneous excitation of multiple QDs with a single wavelength followed by splitting of multiple QD signals into separate detection channels (Fig. 1B,C). This type of multiplex imaging is often difficult to accomplish with standard organic fluorophores because their relatively narrow excitation and broad emission spectra often result in spectral overlap. In agreement with several previous investigations, we show that the broad absorption property of QDs can also be exploited using multiphoton excitation, an imaging method that enables long-term deep imaging in living preparations. The bleaching experiment (Fig. 1D,E), which demonstrates that QDs exhibit superior photostability over long time periods, also suggests that QDs are suited for long-term live imaging experiments.

Cytotoxicity and the potential disruption of cell migration and differentiation by QDs are primary concerns for both in vitro and in vivo experiments. In particular, the constituent heavy metals cadmium and selenide may impact cell survival and proper development. Our LDH release assays (Supplementary Figure S1) and oxidative stress experiments (not shown) suggest that QD loading does not cause any deleterious effect on survival of cell lines in vitro. Furthermore, QD loading of neurospheres has no apparent effect on the differentiation of NSPCs into neuronal and glial lineages of the mammalian nervous system (Fig. 1F–J). Our results also demonstrate that QDs appear to be well tolerated during early embryonic mammalian development. QD-labeled one- and two-cell mouse embryos progressed through successive developmental stages with no obvious abnormalities in cell division (Fig. 2A–D) and developed into fetuses when implanted into pseudo-pregnant dams (Fig. 2F–I). We hypothesize that the heterogeneous levels of QD labeling in the fetuses derived from QD-injected one cell embryos are due to differential proliferation rates between tissues. It is possible, however, that the sorting of QDs to different tissues was stochastic or hampered by deficiencies in detection of small quantities of QDs. Further investigation will be needed to clarify this point. Nevertheless, the compartmentalized segregation of QDs observed during fetal development (Fig. 2A–E) indicates that QD labeling may be particularly useful for embryonic studies to study the formation of nascent primordial layers.

Novel Techniques for QD Delivery to the Developing Nervous System

We developed two techniques to directly QD-label NSPCs in vivo. First, UBM-guided injections of QDs into the parenchyma of the ventral telencephalon directly labeled NSPCs (Fig. 3A). QD-containing cells were found substantial distances away from the initial site of injection 5 days post-injection and had differentiated into neurons, oligodendrocytes, and astrocytes (Fig. 3B–D). The QD-labeled precursors, therefore, retained the capacity to expand into the three main lineages of the forebrain. We then modified in vivo electroporation methods to QD label the CNS precursor cells surrounding the lateral ventricles. Our initial attempts to QD-label NSPCs by means of in utero electroporation showed less than optimal loading of VZ and SVZ cells (Fig. 3E–G), because the QDs were essentially neutral in charge. We found that increasing the negative charge on the QDs by saturating their phospholipid coats with COOH groups substantially increased the labeling efficiency of the neuroepithelial cells. Taking advantage of the high photostability and quantum efficiency exhibited by QDs, high-resolution 3D images of labeled VZ and SVZ neural precursor cells were obtained using multiphoton imaging (Fig. 3J–M). Altogether, these in vivo results suggest that the developmental potential of NSPCs is not adversely affected by QD loading.

The labeling strategies we describe are also applicable to the study of cytogenesis, morphogenesis, migration, and differentiation in any organ system, both pre- and postnatally. For example, targeted delivery and advanced laser-scanning imaging of QDs will enable long-

term tracking of both endogenous and transplanted cells in vivo. Furthermore, our experiments highlight the QD spectral properties and demonstrate how multiplex experiments can be conducted in the developing CNS using multiphoton imaging. The possibility of coupling different species of QDs to an array of bioactive proteins will allow future studies to dynamically image signaling systems in vivo. These new delivery techniques, coupled with the unique and superior fluorescent properties of QDs, constitute a powerful new tool for in vivo studies of mammalian development, tracking of transplanted or host cell populations, and understanding the etiology and diagnosis of disease.

EXPERIMENTAL PROCEDURES

All animal procedures conformed to USDA regulations and were approved by the CNMC and Georgetown University Institutional Animal Care and Use Committees.

Lipofectamine Loading of QD

Neuro2a (N2a) neuroblastoma cells cultured for 24 hr in 12-well plates were loaded with 2.5 ng of QDs (490 nm, 520 nm, 580 nm, and 620 nm) mixed with 4 μl of Lipofectamine (LF) 2000 in 200-μl total volume of Opti-MEM medium (Invitrogen). The medium was changed 8 hr after lipofection. Twenty-four hours later, the cells were imaged using multiphoton excitation at 800 nm and lambda-stack images were collected using Zeiss LSM 510 Meta microscope.

Bleaching Experiment

Imaging was performed using a Zeiss LSM 510 NLO microscope with a ×40 1.3 n.a. Oil/DIC objective. N2a cells were cotransfected with 620-nm QD and EGFP-F plasmid using LF2000 as above. A 7 × 10 μm region of interest was selected containing a QD- and EGFP-labeled membrane. Excitation areas were 0.19 mm^2 for EGFP-F using a 488-nm Argon laser line and 0.25 mm^2 for 620-nm QD using a 633-nm HeNe laser. Peak irradiance was calculated to be 368 mW/mm^2 for the EGFP-F channel and 560 mW/mm^2 for the 620-nm QD channel.

Cytotoxicity Assays

Cell death was quantitatively measured using the Cytox 96 Nonradioactive Cytotoxicity Assay (Promega) using the manufacturer-supplied protocol. N2a cells were cultured in Neurobasal medium (Invitrogen) and loaded with different concentrations of 620-nm QD (12.5–250 ng/ml) and cultured for 6, 12, and 24 hr. Medium was collected from each well at the end of the culture period and assayed for LDH activity (three replicates). For reactive oxygen species measurements, 1 μM of CM-H2DCFDA dye (Molecular Probes) was used to stain 620-nm QD-loaded cells cultured on coverslips in 12-well plates. Cells were loaded for 30 min, washed in dye-free medium, and then imaged using 488-nm excitation and fluorescein isothiocyanate (FITC) configuration using confocal microscopy.

Labeling of Early Stage Mouse Embryos

An in-depth outline of procedures can be found in *Manipulating the Mouse Embryo* 3rd edition (Nagy et al., 2003). Donor mice: Five 3- to 5-week-old FVB donor females were superovulated by injection of pregnant mare serum gonadotropin, followed 24 hr later by human chorionic gonadotropin. One or two cell embryos were obtained 10–20 hr after fertilization.

Mcroinjection, using backfilled injection needles with ~2 μm opening (Sutter Instrument Company Micropipet Puller Model P-97), was performed in FHM medium on a microinjection workstation consisting an Olympus IX70 inverted Microscope, an Eppendorf FemtoJet Microinjector and Eppendorf TransferMan NK2 Micromanipulators. For dual QD injections,

one blastomere of each embryo was injected with 8 femtoliters (0.25 g/L) of 520-nm QDs first, followed by placing all injected embryos in a same orientation. The opposite uninjected blastomere of each embryo was then injected with 0.005 pg of the 620-nm QDs (see Supplementary Tables S1 and S2 for range of concentrations injected). Embryos were allowed to recover in a water-jacketed incubator in a 5% CO_2 environment and analyzed one of four ways: (1) by microscopy at the two-cell stage, (2) by microscopy at the 4- to 8-cell stage after incubating 24–48 hr, (3) by time-lapse multiphoton microscopy during culture on the stage of an LSM 510 NLO microscope, and (4) by microscopy in embryos after implanting them back into pseudopregnant dams.

Implantation of QD-labeled embryos followed the protocol by Nagy et al. (2003). Briefly, foster dams were anesthetized and placed in ventral recumbancy on the lid of a Petri dish so that it could be placed on the stage of a stereoscope. Embryos were transferred to M2 medium and loaded into a transfer pipette. Ovaries were exposed by making a small, 0.5-cm transverse incision 10–15 mm from the spine, posterior to the last rib. The infundibulum was located using a dissecting microscope and a transfer pipette containing QD-injected embryos was inserted into the oviduct. The embryos were then injected into the oviduct.

Differentiation Assay on Neurospheres

Neurospheres were cultured from the ventral telencephalon as previously described (Reynolds and Weiss, 1992). Briefly, ventral telencephalon was freshly dissected out of E14.5 ICR mouse brains and placed in ice-cold Hank's balanced salt solution supplemented with 0.5% (w/v) D-glucose and 25 mM HEPES buffer (Gibco BRL). The tissue was then concentrated by centrifugation and was resuspended in 2 ml of serum-free Neurobasal medium (SFM) containing 2% B27 supplement, 2 mM L-glutamine, 1 mM sodium pyruvate, 100 U/ml penicillin, and 100 μg/ml streptomycin (Gibco BRL). The tissue was triturated using a fire-polished glass pipette to get a single cell suspension. The cells were centrifuged, and the supernatant was removed. The cells were finally resuspended with a brief trituration in 10 ml of proliferation medium (SFM containing 20 ng/ml each of EGF and human recombinant FGF; Stem Cell Technologies), plated at a density of 2×10^6 cells/10 ml in a 100-mm culture dish, and allowed to grow for 3 days in culture.

After two passages (i.e., dissociation and reconstitution into neurospheres), the NSPC-derived neurospheres were allowed to grow for another 4 days before dissociation into single cells. Single cells at a density of 100,000 cells/ well were plated in proliferation medium on poly-L-ornithin (15 μg/ml) and laminin (4 μg/ml) coated glass coverslips in 12-well plates. After 12 hr of continued proliferation, the dissociated cells were loaded with QD by lipofection using LF2000 as above. Eight hours after loading, the medium was changed to differentiation medium (SFM without growth factors) to initiate NSPC differentiation. The cells differentiated for 7 days in vitro.

Immunofluorescence

After fixation in 4% paraformaldehyde (PFA) for 30 min, followed by three (10 min each) washes with 1× phosphate buffered saline (PBS), the cells were permeabilized with 0.2% TritonX-100 in PBS for 10 min followed by 30 min incubation with 5% normal goat serum in 1× PBS. The following antibodies were added at room temperature for 60 min: mouse monoclonal βIII tubulin (1:500; Covance), mouse monoclonal GFAP (1: 500; Chemicon), mouse monoclonal nestin (1:100, Chemicon). In the case of staining for the extracellular NG2 epitope, rabbit polyclonal NG2 (1:500; Chemicon) was added before fixation and permeabilization. The cells were washed with 1× PBS and incubated for 30 min at room temperature with FITC-conjugated secondary antibodies (Southern Biotech). After washing with PBS, the slides were coverslipped with Vectashield containing 4′,6-diamidine-2-

phenylidole-dihydrochloride (DAPI; Vector Laboratories) and images were captured by a digital camera linked to a fluorescence microscope (Olympus).

Ultrasound-Guided Injection of QD

QD were backloaded into an injection needle and, with the aid of ultrasound biomicroscopy (E-Technologies, Bettendorf, IA), ~10 nl (0.25 ng) of 620-nm QDs were injected into the CGE at E13.5. Embryos were killed at E18.5 and perfused with 4% PFA. After perfusion, brains were dissected, post-fixed in PFA for 2–4 hr, cryoprotected in sucrose and embedded in Histoprep (Fisher), and processed for immunocytochemistry with the described antibodies.

Electroporation and Confocal Microscopy

Electroporation was used as described previously (Gal et al., 2006) to transfect VZ cells in utero with QD. Briefly, uterine horns of timed-pregnant dams were exposed by midline laparotomy after anesthetization with ketamine and xylazine. One microliter of QD (75 ng) and/or EGFP-F mixed with 0.03% fast green dye in phosphate buffer was injected intracerebrally using a pulled micropipette through the uterine muscle and amniotic sac. The anode of a Tweezertrode (Genetronics, San Diego, CA) covered in SignaGel (Parker Laboratories, Fairfield, NJ) was placed outside of the uterine muscle over the dorsal telencephalon of the embryo. Three 33-V pulses (50-msec duration; each separated by 950 msec) were applied using a BTX ECM830 pulse generator (Genetronics). After electroporation of all embryos in one uterine horn, the uterus was replaced and the abdominal muscle and skin incisions were closed separately with silk sutures. No embryo mortality was found after electroporation (n = 160), and no dams died from the surgery.

Frozen sections of 20 μm thickness were acquired from electroporated brains that had been fixed with 4% PFA and cryoprotected with 30% sucrose (in PBS). Sections with transfected VZ cells were stained with Hoechst to counterstain DNA. Z-stack images of VZ cells were prepared from 10 optical sections spaced 1 μm apart using confocal and multiphoton imaging.

Supplementary Material

Refer to Web version on PubMed Central for supplementary material.

ACKNOWLEDGMENTS

The authors thank Melissa Shaya and Carlos Benitez for technical assistance. T.F.H. and B.S.B. were funded by NINDS; J.G.C. received a MRD-DRC New Investigator Award from the Children's Research Institute, Washington DC, and funding by NIDA; B.S.B. was funded by NICHD; and J.R.S. received an award from the American Association of Neurological Surgeons/Congress of Neurological Surgeons.

Grant sponsor: the CNMC Board of Visitors; Grant sponsor: NINDS; Grant number: NS051852; Grant number: NS27054 Grant sponsor: National Alliance for Autism Research; Grant sponsor: the Children's Research Institute, Washington DC; Grant sponsor: NIDA; Grant number: DA020140; Grant sponsor: NICHD; Grant number: HD007459; Grant sponsor: the American Association of Neurological Surgeons/Congress of Neurological Surgeons; Grant sponsor: Evident Technologies.

REFERENCES

Ballou B, Lagerholm BC, Ernst LA, Bruchez MP, Waggoner AS. Non-invasive imaging of quantum dots in mice. Bioconjug Chem 2004;15:79–86. [PubMed: 14733586]

Bruchez M Jr, Moronne M, Gin P, Weiss S, Alivisatos AP. Semiconductor nanocrystals as fluorescent biological labels. Science 1998;281:2013–2016. [PubMed: 9748157]

Chan WC, Nie S. Quantum dot bioconjugates for ultrasensitive nonisotopic detection. Science 1998;281:2016–2018. [PubMed: 9748158]

Clapp AR, Medintz IL, Mattoussi H. Forster resonance energy transfer investigations using quantum-dot fluorophores. Chemphyschem 2006;7:47–57. [PubMed: 16370019]

Dahan M, Levi S, Luccardini C, Rostaing P, Riveau B, Triller A. Diffusion dynamics of glycine receptors revealed by single-quantum dot tracking. Science 2003;302:442–445. [PubMed: 14564008]

Dubertret B, Skourides P, Norris DJ, Noireaux V, Brivanlou AH, Libchaber A. In vivo imaging of quantum dots encapsulated in phospholipid micelles. Science 2002;298:1759–1762. [PubMed: 12459582]

Gal JS, Morozov YM, Ayoub AE, Chatterjee M, Rakic P, Haydar TF. Molecular and morphological heterogeneity of neural precursors in the mouse neocortical proliferative zones. J Neurosci 2006;26:1045–1056. [PubMed: 16421324]

Gao X, Cui Y, Levenson RM, Chung LW, Nie S. In vivo cancer targeting and imaging with semiconductor quantum dots. Nat Biotechnol 2004;22:969–976. [PubMed: 15258594]

Han M, Gao X, Su JZ, Nie S. Quantum-dot-tagged microbeads for multiplexed optical coding of biomolecules. Nat Biotechnol 2001;19:631–635. [PubMed: 11433273]

Hoshino A, Fujioka K, Oku T, Nakamura S, Suga M, Yamaguchi Y, Suzuki K, Yasuhara M, Yamamoto K. Quantum dots targeted to the assigned organelle in living cells. Microbiol Immunol 2004;48:985–994. [PubMed: 15611617]

Jaiswal JK, Goldman ER, Mattoussi H, Simon SM. Use of quantum dots for live cell imaging. Nat Methods 2004;1:73–78. [PubMed: 16138413]

Jaiswal JK, Simon SM. Potentials and pitfalls of fluorescent quantum dots for biological imaging. Trends Cell Biol 2004;14:497–504. [PubMed: 15350978]

Kim S, Lim YT, Soltesz EG, De Grand AM, Lee J, Nakayama A, Parker JA, Mihaljevic T, Laurence RG, Dor DM, Cohn LH, Bawendi MG, Frangioni JV. Near-infrared fluorescent type II quantum dots for sentinel lymph node mapping. Nat Biotechnol 2004;22:93–97. [PubMed: 14661026]

Kirchner C, Liedl T, Kudera S, Pellegrino T, Munoz Javier A, Gaub HE, Stolzle S, Fertig N, Parak WJ. Cytotoxicity of colloidal CdSe and CdSe/ZnS nanoparticles. Nano Lett 2005;5:331–338. [PubMed: 15794621]

Larson DR, Zipfel WR, Williams RM, Clark SW, Bruchez MP, Wise FW, Webb WW. Water-soluble quantum dots for multiphoton fluorescence imaging in vivo. Science 2003;300:1434–1436. [PubMed: 12775841]

Levene MJ, Dombeck DA, Kasischke KA, Molloy RP, Webb WW. In vivo multiphoton microscopy of deep brain tissue. J Neurophysiol 2004;91:1908–1912. [PubMed: 14668300]

Medintz IL, Uyeda HT, Goldman ER, Mattoussi H. Quantum dot bioconjugates for imaging, labelling and sensing. Nat Mater 2005;4:435–446. [PubMed: 15928695]

Michalet X, Pinaud FF, Bentolila LA, Tsay JM, Doose S, Li JJ, Sundaresan G, Wu AM, Gambhir SS, Weiss S. Quantum dots for live cells, in vivo imaging, and diagnostics. Science 2005;307:538–544. [PubMed: 15681376]

Nagy, A.; Vintersten, K.; Behringer, R. Manipulating the mouse embryo: a laboratory manual. Cold Spring Harbor, NY: Cold Spring Harbor Laboratory Press; 2003. p. 764

Nan X, Sims PA, Chen P, Xie XS. Observation of individual microtubule motor steps in living cells with endocytosed quantum dots. J Phys Chem B 2005;109:24220–24224. [PubMed: 16375416]

Pathak S, Cao E, Davidson MC, Jin S, Silva GA. Quantum dot applications to neuroscience: new tools for probing neurons and glia. J Neurosci 2006;26:1893–1895. [PubMed: 16481420]

Reynolds BA, Weiss S. Generation of neurons and astrocytes from isolated cells of the adult mammalian central nervous system. Science 1992;255:1707–1710. [PubMed: 1553558]

Rieger S, Kulkarni RP, Darcy D, Fraser SE, Koster RW. Quantum dots are powerful multipurpose vital labeling agents in zebrafish embryos. Dev Dyn 2005;234:670–681. [PubMed: 16110511]

Rosenthal SJ, Tomlinson I, Adkins EM, Schroeter S, Adams S, Swafford L, McBride J, Wang Y, DeFelice LJ, Blakely RD. Targeting cell surface receptors with ligand-conjugated nanocrystals. J Am Chem Soc 2002;124:4586–4594. [PubMed: 11971705]

Shiohara A, Hoshino A, Hanaki K, Suzuki K, Yamamoto K. On the cyto-toxicity caused by quantum dots. Microbiol Immunol 2004;48:669–675. [PubMed: 15383704]

Soltesz EG, Kim S, Laurence RG, DeGrand AM, Parungo CP, Dor DM, Cohn LH, Bawendi MG, Frangioni JV, Mihaljevic T. Intraoperative sentinel lymph node mapping of the lung using near-infrared fluorescent quantum dots. Ann Thorac Surg 2005;79:269–277. [PubMed: 15620956] discussion 269–277.

Soltesz EG, Kim S, Kim SW, Laurence RG, De Grand AM, Parungo CP, Cohn LH, Bawendi MG, Frangioni JV. Sentinel lymph node mapping of the gastro-intestinal tract by using invisible light. Ann Surg Oncol 2006;13:386–396. [PubMed: 16485157]

Stroh M, Zimmer JP, Duda DG, Levchenko TS, Cohen KS, Brown EB, Scadden DT, Torchilin VP, Bawendi MG, Fukumura D, Jain RK. Quantum dots spectrally distinguish multiple species within the tumor milieu in vivo. Nat Med 2005;11:678–682. [PubMed: 15880117]

Voura EB, Jaiswal JK, Mattoussi H, Simon SM. Tracking metastatic tumor cell extravasation with quantum dot nanocrystals and fluorescence emission-scanning microscopy. Nat Med 2004;10:993–998. [PubMed: 15334072]

Vu TQ, Maddipati R, Blute TA, Nehilla BJ, Nusblat L, Desai TA. Peptide-conjugated quantum dots activate neuronal receptors and initiate downstream signaling of neurite growth. Nano Lett 2005;5:603–607. [PubMed: 15826094]

Wu X, Liu H, Liu J, Haley KN, Treadway JA, Larson JP, Ge N, Peale F, Bruchez MP. Immunofluorescent labeling of cancer marker Her2 and other cellular targets with semiconductor quantum dots. Nat Biotechnol 2003;21:41–46. [PubMed: 12459735]

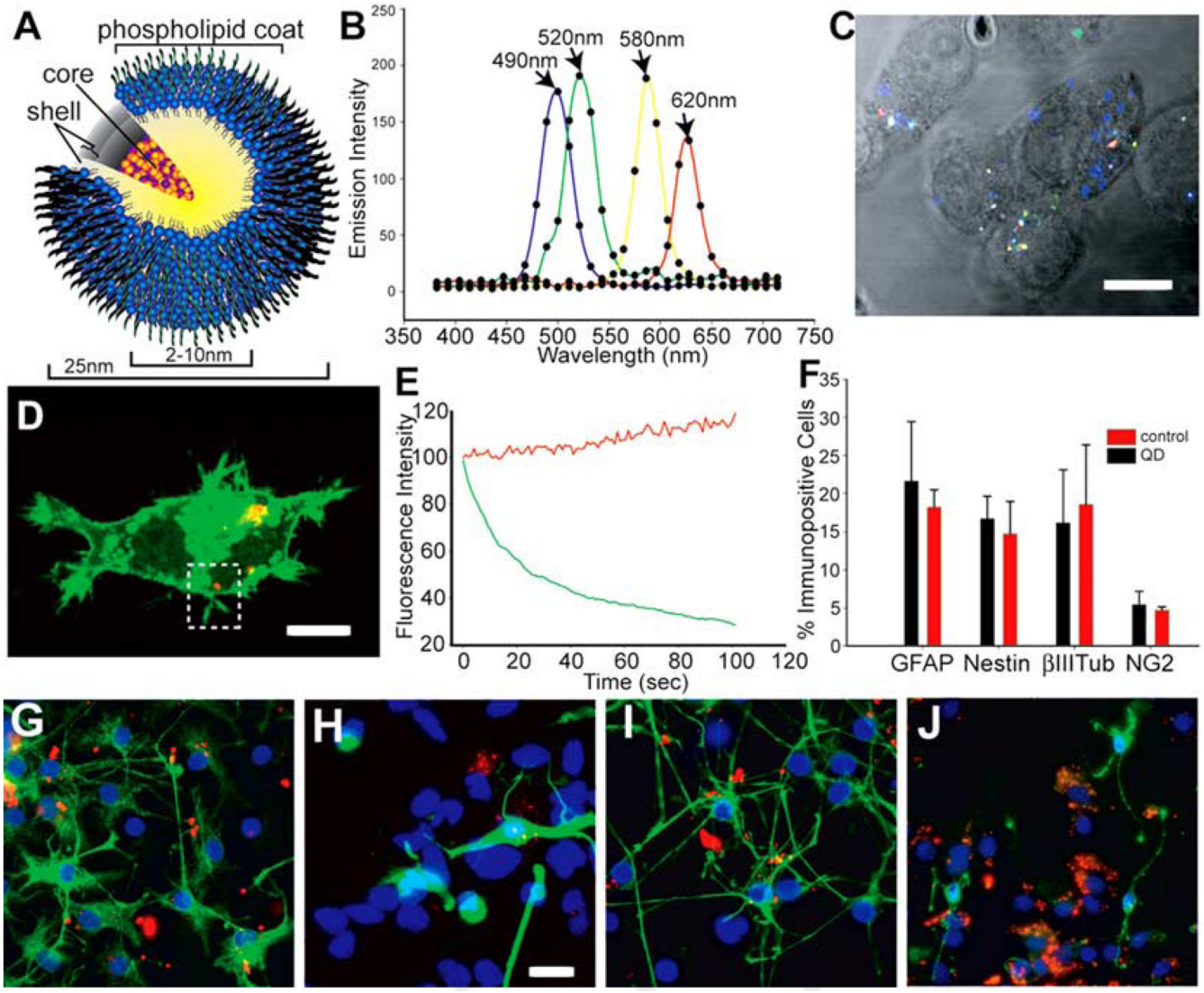

Fig. 1. The composition and spectral characteristics of quantum dots

A: The quantum dots (QDs) have CdSe core/ZnS shell covered by a phospholipid coat to which ligands and amine and carboxy groups can be added to functionalize the QDs. **B,C**: N2a cells were loaded with an equimolar mix of 490-nm, 520-nm, 580-nm, and 620-nm QDs in vitro using Lipofectamine (LF) 2000. Twenty-four hours later, the cells were imaged using multiphoton excitation at 800 nm and detected with Zeiss Meta detector. The emission fingerprints of the four QDs are graphed in B, and an unmixed lambda stack image is shown in C. **D,E**: N2a cells were simultaneously loaded with 620-nm QDs and transfected with farnesylated enhanced green fluorescence protein (EGFP-F) using LF2000. The region of interest (dotted area) in D was scanned 120 times using a 488-nm argon laser to excite EGFP-F and a 633-nm HeNe laser for the QD excitation. Traces of fluorescence intensity vs. time in E demonstrate that the QD emission increased slightly during repetitive illumination while EGFP fluorescence faded. F–J: To track the differentiation of QD-loaded cells in culture, neurospheres cultured from embryonic day (E) 14.5 ventral telencephalon were dissociated and the resulting cells were labeled with 620-nm QD using LF2000 for 1 day in proliferation medium. **G–J**: After 7 days of subsequent culture in differentiation medium, the cells were immunostained for nestin (G), βIII-tubulin (H), glial fibrillary acidic protein (GFAP, I) and

NG2 (J). **F**: No significant difference in the percentage of immunopositive cells for any antigen was found after neural stem cell differentiation (F). Scale bars = 10μm in C,D, 15μm in G–J.

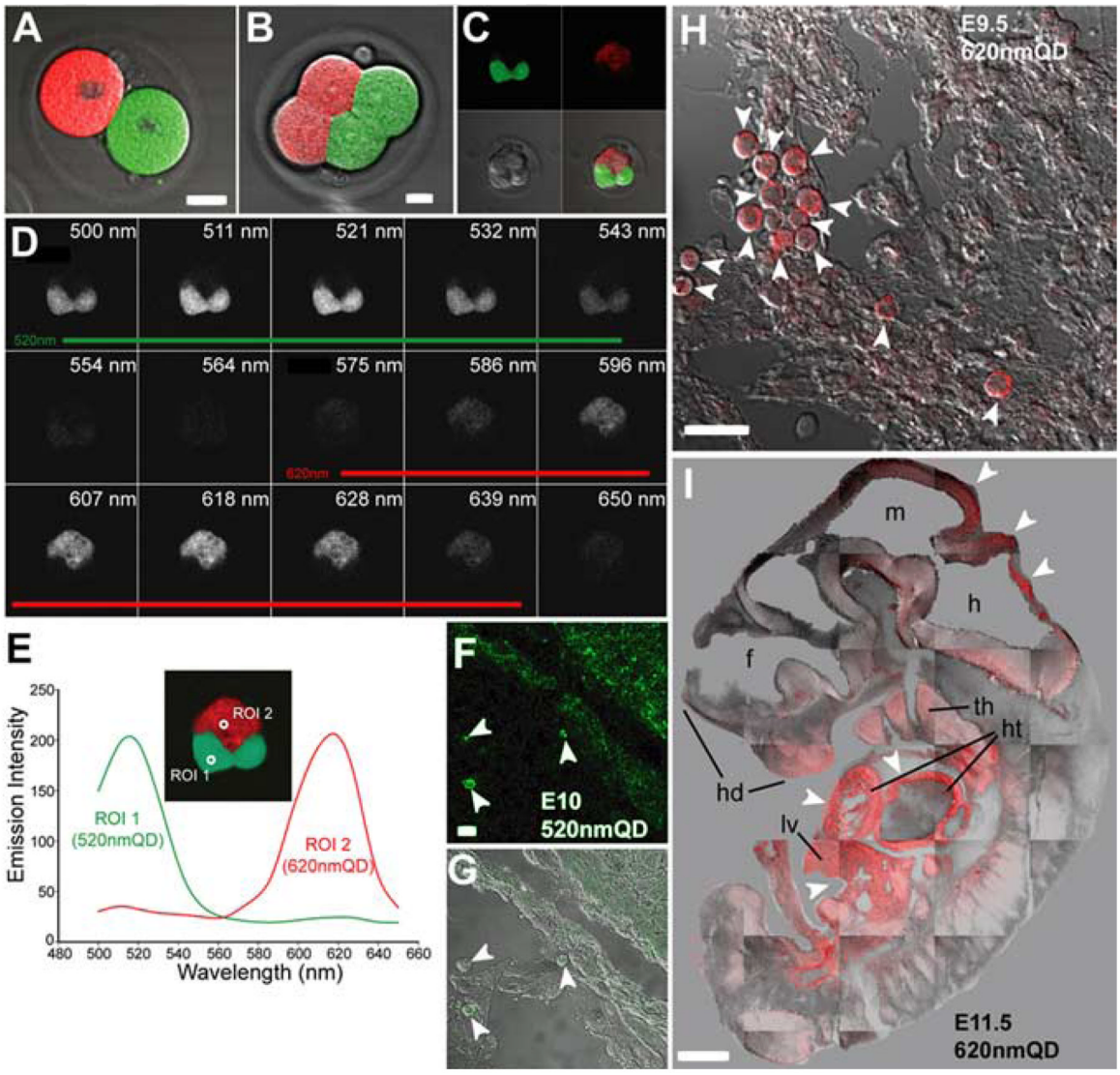

Fig. 2. Quantum dot (QD) labeling of early mouse embryos does not alter fetal development

A: Two-cell stage mouse embryos injected with 520-nm and 620-nm QDs in vitro were allowed to divide for 1–2 days in culture. **B,C**: Four-cell (B) and eight-cell (C) stage embryos developed with compartmentalized segregation of QD into daughter cells during development demonstrating there was no mixing of QD during cell division. **D**: Lambda stack image illustrates the spectral characteristics of each QD. **E**: Emission fingerprints of 520-nm and 620-nm QD. **F–I**: One- and two-cell stage 520-nm or 620-nm QD-injected mouse embryos were implanted into pseudo-pregnant dams for 9.5 to 11.5 days of in utero development. All embryonic tissues appeared to contain QDs, although there was uneven labeling with some tissues containing a higher density of QD. E–G: For example, cells in the umbilical region of an embryonic day (E) 10 fetus injected with 520-nm QD (arrowheads in F,G) had more QD labeling than the underlying epithelial cells. H: Another E9.5 fetus labeled at the one-cell stage with 620-nm QD, exhibited some heavily labeled ventricular pericardial cells (arrowheads) while other neighboring cells possessed much lower QD labeling. I: In an E11.5 embryo where 620-nm QD were loaded into one-cell at the two-cell stage, there was asymmetrical labeling of body tissues by QDs. There was much higher labeling (arrowheads) in the liver (lv), cardiac

primordium (ht), thymus (th), and hindbrain (h) compared with other tissues. hd, head; f; forebrain; m, midbrain. Scale bars = 5 μm in A,B; 15 μm in F,G; 20 μ m in H; 0.5 mm in I.

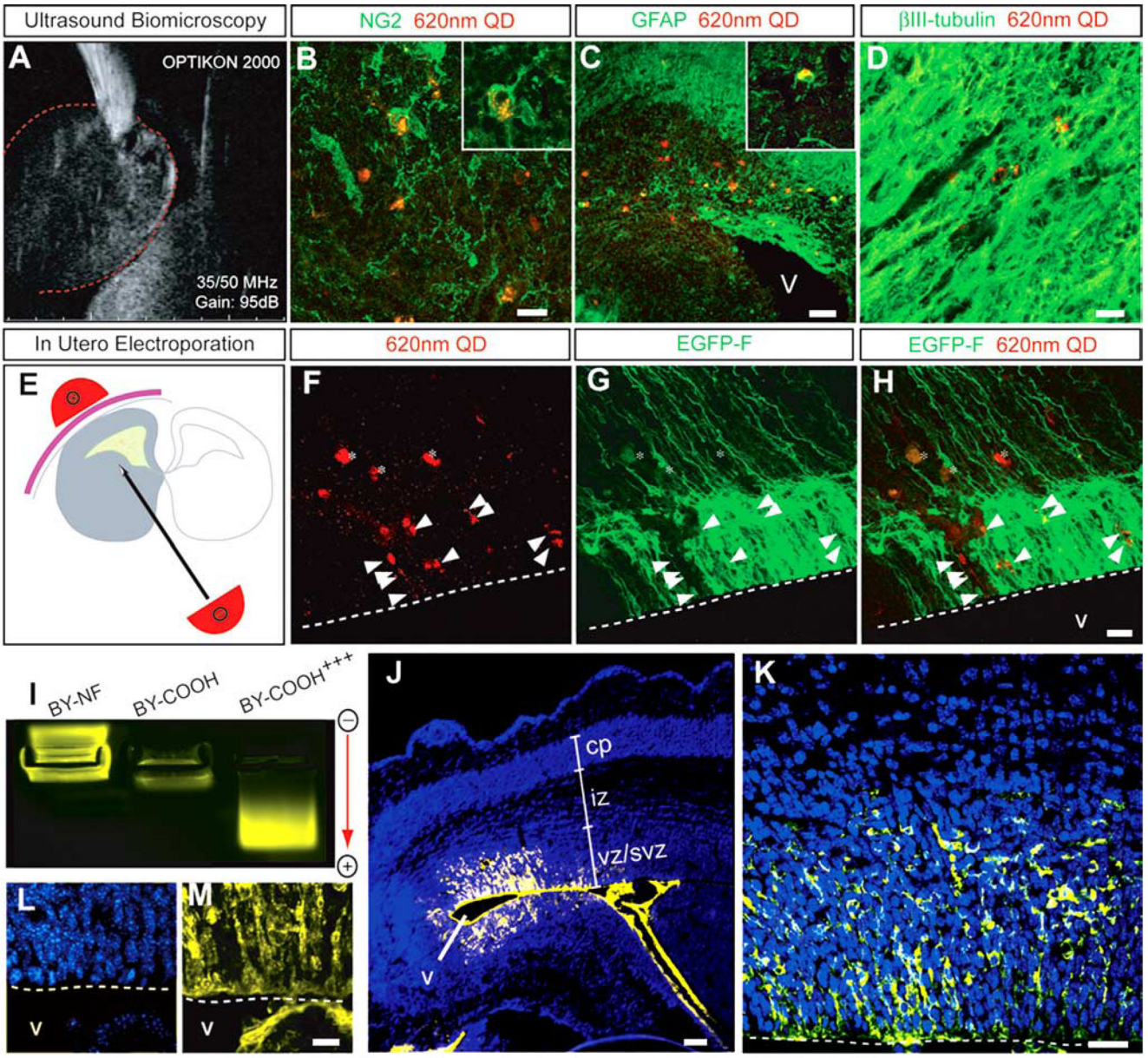

Fig. 3. A–M: Direct in utero labeling of cells with quantum dot (QD) using ultrasound biomicroscopy (A–D) and electroporation (E–M)

A: The 620-nm QDs were injected into the caudal ganglionic eminence of embryonic day (E) 13.5 mouse brains with the aid of high-resolution ultrasound biomicroscopy. **B–D**: In a coronal view of E18.5 developing cerebral cortex, intracellular labeling of QD was observed in $NG2^+$ oligodendrocytes (B), $GFAP^+$ astrocytes (C), and $\beta III\text{-tubulin}^+$ neurons (D). **E**: The lateral ventricles of E14.5 mouse embryos were injected in utero with a mix of 620-nm QD and farnesylated enhanced green fluorescence protein (EGFP-F) plasmid followed by electroporation with 3× 33-volt electrical pulses. **F**: Twenty-four hours later, QD labeling was found in the ventricular zone (VZ) and subventricular zone (SVZ) cells lining the lateral ventricle (arrowheads) and in the parenchymal blood vessels overlying the germinal zones (asterisks). **G**: The areas with QD-containing cells also had many EGFP-transfected cells. **H**: Overlay of F and G. **I**: Agarose gel electrophoresis of 580-nm QD in various conformations:

nonfunctionalized (NF), functionalized (20–30% saturation) by carboxy groups (COOH), and high saturation by carboxy groups (COOH+ + +). **J,K**: In utero electroporation of E16.5 embryos with carboxy-saturated 580-nm QD increases the labeling efficiency with many VZ and SVZ neural precursor cells loaded with QD. K: A high-magnification confocal optical section demonstrates robust QD labeling (yellow) of cells surrounding the lateral ventricle. **L,M**: Collapsed z-stack images of 10 optical sections spaced 1 μm apart. The blue label is Hoechst nuclear stain. Dotted lines demarcate the ventricular boundary. vz/svz, ventricular and subventricular zones; iz, intermediate zone; cp, cortical plate; v, ventricle. Scale bars = 10 μm in B,D, 20 μm in C,F–H.